Advances in Sample Preparation 12 (2024) 100134

Contents lists available at ScienceDirect

Advances in Sample Preparation

journal homepage: www.elsevier.com/locate/sampre

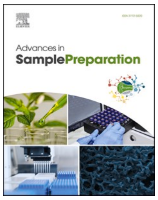

Microextraction by packed sorbent: Introducing a novel hybrid silica-based chitosan-graphene oxide biosorbent for the evaluation of pesticides and antibiotics in food matrices

Rafael O. Martins, Fernando M. Lanças *

Instituto de Química de São Carlos, Universidade de São Paulo, São Carlos, SP 13566-590, Brazil

ARTICLE INFO

Keywords:
Pesticides
Antibiotics
Microextraction by packed sorbent
Food analysis
Graphene oxide
Chitosan

ABSTRACT

This study introduces a novel silica-graphene oxide@chitosan (SiGO@CS) material as a packed biosorbent for microextraction by packed sorbent (MEPS), followed by liquid chromatography-tandem mass spectrometry (LC-MS/MS) analysis of pesticides (atrazine and thiamethoxam) and antibiotics (ceftiofur and sulfonamide) in food samples. The graphene-based aerogel was modified with varying percentages of silica-graphene oxide/chitosan (w/w) and characterized to confirm successful chitosan incorporation. Optimization of the MEPS protocol, using 2^{4-1} and 2^3 experimental designs, identified draw/eject and washing cycles as the most influential parameters for extraction efficiency. The SiGO@CS biosorbent with 80 % CS/SiGO (w/w) exhibited superior extraction efficiency compared to other ratios and commercial sorbents. The method demonstrated excellent linearity for all analytes ($R^2 > 0.9900$), with low limits of detection (LOD) and quantification (LOQ) ranging from 0.020 to 0.045 $\mu g\ L^{-1}$ and 0.045 to 1.0 $\mu g\ L^{-1}$ for pesticides, respectively, and 5 to 15 $\mu g\ L^{-1}$ and 15 to 20 $\mu g\ L^{-1}$ for antibiotics, respectively. Trueness values were within 82 % to 109 %. The method's green credentials were confirmed using AGREEprep and the Green Analytical Procedure Index (GAPI) approach, highlighting sorbent reusability (over 15 times) and rapid analytical throughput (5 min per sample) with low use of pre-treated sample extract volume (500 μL). The application to local corn, tomato, and milk samples confirmed the detection and quantification of thiamethoxam and atrazine at concentrations above the recommended ingestion per day for one sample of tomato and corn out of the three samples analyzed. Furthermore, using the novel SiGO@CS biosorbent in the MEPS protocol offers a green, high-performance analytical alternative to traditional sorbent phases, with the potential for evaluating trace levels of pesticides and antibiotics in food matrices.

1. Introduction

Over the past century, population growth has the imperative to ensure sufficient food resources to sustain a dignified and high-quality human existence [1]. Consequently, the application of chemical compounds in agricultural practices, notably antibiotics, and pesticides, has evolved into a pervasive approach aimed at augmenting food production to address the escalating global demand for these indispensable resources [2,3]. Nevertheless, literature has documented the adverse effects on human health associated with the presence of these compounds in food [3–5]. Furthermore, the indiscriminate application of chemicals throughout the growth post-processing stages presents a formidable challenge in detecting these compounds at low concentration levels [6]. Among these concerns, food quality and safety are paramount, underscoring the imperative for a thorough analysis of food residues [7]. Consequently, there is a pressing need to deploy analytical methodologies to accurately assess the presence of chemical residues in these intricate matrices.

Liquid chromatography (LC), as well as its coupling with tandem mass spectrometry (LC-MS/MS) strategies, are typically utilized to detect and quantity trace-level concentrations of residues in food samples [6]. Nonetheless, the inherent complexity of these matrices renders direct analysis via various analytical instruments unfeasible, necessitating specific sample preparation steps to ensure that the method's statistical performance meets established requirements [8]. To address the significant drawbacks of traditional sample preparation techniques, miniaturized methodologies have evolved over decades, opening up new possibilities for residue assessment in food matrices [8,9]. Furthermore,

---

* Corresponding author.
E-mail address: flancas@iqsc.usp.br (F.M. Lanças).

https://doi.org/10.1016/j.sampre.2024.100134
Received 19 August 2024; Received in revised form 29 October 2024; Accepted 3 November 2024

the miniaturized landscape has embraced critical principles of green analytical chemistry (GAC), striving to introduce analytical approaches that minimize solvent consumption and reduce waste generation [9]. In this context, microextraction by packed sorbent (MEPS) has emerged as a promising miniaturized solid-based technology capable of assessing multiple residues in complex matrices [8]. Typical advantages of this analytical strategy typically include minimal sorbent masses and reduced sample/solvent volumes, culminating in an easy and cost-effective methodology. Consequently, it offers boundless potential for seamless integration into daily analytical protocols, facilitating high-throughput analyses [10,11]. Moreover, significant advancements have been achieved in MEPS, particularly in developing new selective and cost-effective sorbent phases [12,13]. These innovations enhance the method's ability to analyze various target analytes, such as food samples, within a wide range of matrices.

Carbon-based materials have garnered significant scientific attention due to their characteristics, including different and unexplored allotropic forms [12]. Graphene (G) emerged as a leading material for fabricating sorbents in 2003, owing to its large specific surface area and remarkable stability [14]. These materials have demonstrated remarkable pollutant adsorption capabilities across various matrices, especially in environmental samples such as natural water sources [15,16]. Following the groundbreaking introduction of G materials, its precursor, graphene oxide (GO), has also showcased significant promise in the scientific field of sample preparation [12]. GO materials typically display a notably high surface area, a π-electron system, and a wealth of oxygen-containing functional groups [17]. Their utilization as adsorbent materials for pollutant analysis has been extensively documented in the literature, showcasing their remarkable suitability for residue assessment across various matrices [18].

On the other hand, a prevalent drawback arises from the robust π-π interaction among the GO sheets, which often leads to aggregation. Consequently, this minimizes the surface area and diminishes adsorption efficiency, resulting in poor dispersion in aqueous media [17]. Furthermore, numerous researchers have concentrated on functionalization and the synergistic combination of GO with other materials to overcome the typical limitations associated with the sole use of GO materials.

Chitosan (CS) stands out as a biopolymer renowned for its eco-friendly adsorbent properties, owing to its unique characteristics, including biodegradability, non-toxicity, and physicochemical features [19]. The successful immobilization of graphene oxide and chitosan (GO/CS) relies on the abundant presence of -OH and -NH_2 groups, which facilitate effective electrostatic interactions and hydrogen bonding with functional groups on GO [17,20,21]. This interaction enables the anchoring of CS within the GO system to improve GO applications. Another factor contributing to the ideal compatibility between GO and CS is that the biopolymer exhibits relatively poor thermal stability and mechanical properties. However, when combined with GO, these crucial shortcomings are significantly enhanced [17,22]. Simultaneously, the utilization of CS serves as a stabilizing agent for the GO sheets, effectively addressing the previously mentioned aggregation issue in this newly derived absorbent material [17]. Additionally, just a few literature reports demonstrate the use of GO-based materials in MEPS applications [23]. This can be attributed to the natural nanosheet morphology of G and its resulting large surface area, which exacerbates the backpressure issue with the MEPS syringe, thereby impacting the application of these materials in this analytical method [17,18]. Despite this, our research group has demonstrated that the combination of aminopropyl silica (Si) through covalent bonding with GO (SiGO) can overcome this drawback, thus enabling the utilization of the material in MEPS protocols [23,24]. Hence, this study endeavors to develop a carbon-based material by the combination of CS biopolymer and GO sheets with later covalent bonding with Si serving as a sorbent material for the evaluation of pesticides and antibiotics in food samples via microextraction by packed sorbent followed by liquid chromatography-tandem mass spectrometry (MEPS LC-MS/MS). This is the first time in the literature that a silica-graphene oxide@chitosan biomaterial (SiGO@CS) in MEPS methodology for assessing selected antibiotics and pesticides in food samples has been presented.

2. Materials and methods

2.1. Materials

Methanol (MeOH), acetonitrile (ACN) LC grade, and sodium chloride were purchased from JT Baker (Phillipsburg, USA). Sodium nitrate, sodium sulfate, potassium permanganate, graphite (<20 μm synthetic), and CS with a medium molecular weight (200–800 cP and >75 % deacetylation chitin, Poly(D-glucosamine), 1-ethyl-3-(3-dimethyl aminopropyl) carbodiimide hydrochloride (EDC), hydroxisuccinimide 97 % (NHS), glutaraldehyde solution (25 % in H_2O), acetic acid were acquired from Sigma-Aldrich (St. Louis, USA). Acetone was purchased from TEDIA (Fairfield, USA). Pesticides and antibiotics standards (>98 % purity) thiamethoxam (THI), atrazine (ATR), ceftiofur (CEF), and sulfonamide (SUL) were obtained from Sigma-Aldrich (St. Louis, USA). Sulfuric acid, 97.9 %, was purchased from Êxodo Científica (Sumaré, Brazil). Si from different particle diameters 40–70 μm, citric acid, and sodium phosphate dibasic were acquired from Sigma-Aldrich (St. Louis, USA). Amino (NH_2) and Bond Elut Silica sorbent phases were obtained from JT Baker (Phillipsburg, USA). Ultrapure water was obtained from the Millipak ® Express 40 equipment (Merck Millipore, Burlington, Massachusetts, USA).

2.2. GO synthesis and supporting on silica particles (SiGO)

GO was synthesized using a modified Hummers method [25], involving the reaction of graphite, sodium nitrate, and potassium permanganate within a concentrated sulfuric acid reaction medium. The resulting GO material was washed until reaching a neutral pH and freeze-dried using an FR-Drying Digital Unit MODULYOD-115 (Thermo Fisher, Waltham, USA) to obtain the final GO nanoparticles. The supporting of GO onto Si particles was proposed according to an adapted protocol from earlier investigations conducted by our research group [26,27]. For this purpose, 40 mg of GO was dispersed in 80 mL of water and subjected to ultrasonic treatment for 1 h to ensure complete solubilization. Subsequently, a solution containing 0.750 μL of 0.10 mol l^{-1} EDC and 0.05 mol l^{-1} NHS was prepared and stirred for 30 min to activate the GO nanosheets. In the next step, 1 g of Si was added to the solution and stirred for 4 h The obtained SiGO material was then centrifuged with a Rotina 380 (Nova Anallitica, São Paulo, Brazil) equipment (5000 rpm/5 min) equipment and washed three times with MeOH, ACN, and water alternately (5000 rpm/5 min). The resulting material was subsequently subjected to an overnight freeze-drying process before being stored under ambient conditions.

2.3. Synthesis of the SiGO@CS biosorbent

The SiGO material previously acquired was employed to synthesize the SiGO@CS biosorbent. In the synthesis procedure, varying proportions of CS to SiGO (20, 50, and 80 % w/w) were precisely measured and dissolved in a 10 mL acetic acid solution (1 % v/v). The resulting solution underwent ultrasonication for 15 min and then stirred for 30 min to ensure complete CS solubilization. Furthermore, 5 g of SiGO was introduced into the CS solution and stirred for 10 min. The mixture was gradually heated to 50 °C and stirred for 2 h when 200 μL of a glutaraldehyde solution (25 % in H_2O) was added to the reaction medium to crosslinker between SiGO and CS. The resulting solution was maintained at the same temperature and stirring conditions for 1 h Afterward, the solution was centrifugated and underwent three rounds of washing with acetone. The resultant material, SiGO@CS-GLU, was then submitted to a freeze-drying process overnight and subsequently stored under ambient conditions for later MEPS assays (**Fig. S1 in the supplementary material**). For comparison evaluation, aerogels of GO/CS, pure CS, SiGO@CS-GLU 20, 50, and 80 % (CS/SiGO w/w), and SiGO@CS with no glutaraldehyde addition were also prepared and submitted to characterization assays.

2.4. Materials characterization

The synthesized materials underwent characterization assays to evaluate a spectrum of physicochemical properties. Fourier Transform Infrared (FTIR) spectroscopy was employed, operating within the spectral range of 600–4000 cm^{-1}, utilizing the Tensor 27 instrument (Bruker, Massachusetts, USA). Moreover, Scanning Electron Microscopy (SEM) and Energy-dispersive X-ray spectroscopy (EDX) analysis investigated the sorbents' surface morphology and elemental composition. Both studies used an LEO 440 scanning electron microscope (LEO Electron Microscopy Ltd., Cambridge, England) with an acceleration potential of 15 kV, magnifying 500 to 2000x.

2.5. Samples and stock solutions

This study proposed the assessment of selected pesticides and antibiotics in food samples, including ATR, THI, SUL, and CEF. **Table S1** shows some physicochemical properties of the selected analytes. Stock standard solutions of these analytes were prepared in ACN across various concentration ranges (10 to 500 µg l^{-1}) and stored at a controlled temperature (4 °C). The food samples (corn, tomato, milk) used for optimization and validation were obtained from local markets in São Carlos, São Paulo, Brazil (Latitude: −22.0154; Longitude: −47.8911) and stored under controlled temperature (4 °C) conditions.

To prepare corn and tomato samples, this study used an adapted previous report from our research group [28] which has demonstrated an effective approach for extracting pesticides from solid-based food samples. For this aim, crushed corn and tomato samples (1.0 g) were spiked with the selected pesticides (THI and ATR at 100 µg l^{-1}), dried, and stored in a freezer environment (−10 °C). The samples were first resuspended in 5 mL of ACN, stirred for 6 h, and then homogenized in an ultrasonic bath for 1 h at 45 °C. At this stage, 1.5 g of sodium sulfate was added to the tomato extract solution to remove water content, as outlined by Hegazy et al. [29]. Afterward, they were centrifuged at 5.000 rpm for 10 min. The resulting supernatant was then dried under a N_2 flow. For the MEPS procedure, the resuspended extracts in 1 mL of water were homogenized using ultrasound for 10 min and subsequently subjected to extraction. For the milk sample preparation, the protocol described by Maciel et al. [27] was used to prevent frit obstruction during the MEPS procedure. First, 2 mL of trifluoroacetic acid (20 % v/v) was added to 5 mL of the spiked milk sample (CEF and SUL at 300 µg l^{-1}) and mixed using a vortex apparatus for 30 s. Then, 20 mL of McIlvaine buffer solution/EDTA (0.05 M) was added to the sample solution and centrifuged at 5000 rpm for 5 min. The resulting supernatant was separated and applied to the MEPS extraction. For the MEPS procedure in milk samples, both the conditioning phase (500 µL) and the McIlvaine buffer solution/EDTA (1000 µL) were passed through the MEPS sorbent.

The developed MEPS LC-MS/MS method was applied to analyze pesticides and antibiotics in food samples obtained from local markets across different regions of São Paulo, Brazil. The detected concentrations were compared with regulatory standards to validate the applicability of the reported biosorbent used in the MEPS extraction for food samples.

2.6. MEPS procedure optimization

Although the MEPS procedure presents remarkable operational simplicity, numerous intrinsic parameters can significantly impact its performance. To have more profound insights into the influence of these parameters on MEPS efficacy, this study suggested employing two experimental strategies. The MEPS optimization procedure was performed in spiked food sample solutions at 100 µg l^{-1}. Initially, 7 mg of the SiGO@CS-GLU 80 % (CS/SiGO w/w) sorbent was carefully packed into the barrel insert and needle (BIN) and sealed with frit (VICI ®10SR2–10) (Houston, USA) and placed in a 500 µL Hamilton syringe (Reno, USA). Therefore, a preliminary factorial design (2^{4-1}) was executed to assess the impact of sample pH, ionic strength (NaCl w/v%), choice of desorption solvent, and desorption solvent volume. These parameters were prioritized for evaluation due to their anticipated significant influence on overall performance. For this first evaluation, MEPS conditions were set as follows: six draw/eject cycles with 500 µL of food samples (sampling), four washes with 250 µL of ultrapure water to remove potential interferents presented in the matrices, and ten desorption cycles with the desorption solvent evaluated by the factorial design. Table 1**A** summarizes the evaluated parameters of the 2^{4-1} factorial design.

Table 1
Variables levels optimized by factorial design; **1A** - Factorial Design 2^{4-1} for the optimization of the sample pH, ionic strength, desorption solvent, and desorption solvent volume; **1B** - Factorial design 2^3 with a center point used in the MEPS cycles (draw eject, desorption, and washing cycles) optimization.

1A - Factorial Design 2^{4-1}					
Variable Levels	**−1**			**+1**	
Sample pH	3			7	
Ionic strength % NaCl (w/v)	0 %			20 %	
Desorption Solvent	ACN			MeCN	
Desorption Solvent volume (µL)	50			100	
1B - Factorial Design 2^3 with a center point					
Variable Levels	**−1**		**+1**		**+1**
Draw/Eject Cycles	3	6		9	
Desorption Cycles	8	10		12	
Washing Cycles	2	4		6	

After setting the best conditions of the 2^{4-1} factorial design, this study also evaluated the number of MEPS cycles, encompassing draw/eject, desorption using ACN and methanol/acetonitrile (MeCN) 50/50 % v/v, and washing stages with water, utilizing a factorial design (2^3) with a replicated center point ($n = 3$). Table 1**B** shows the evaluation of the 2^3 parameters described in the study. The subsequent MEPS cycles (conditioning/regeneration and sorbent drying) were also executed to avoid the carryover effect and ensure the thorough dryness of the sorbent. The final MEPS extraction product was dried using a SpeedVac SPD120 from Thermo Scientific (Massachusetts, USA) and stored in a controlled temperature environment for subsequent LC-MS/MS analysis.

2.7. LC-MS analysis

LC-MS/MS analysis of the MEPS optimization, validation, and application to food samples was conducted utilizing an ultra-performance liquid chromatography-tandem mass spectrometry (UPLC-MS/MS) system. This system comprised an ACQUITY Ultra Performance instrument (Waters, Milford, USA), outfitted with an ACQUITY UPLC® M-Class BEH C18 130 Å column (1.7 µm x 300 mm x 100 µm; Waters, Waters, Milford, USA), an ACQUITY UPLC micro-sample manager (Waters, Milford, USA), and a UPLC micro-binary solvent manager coupled to a XEVO TQ MS (Waters, Milford, USA) tandem mass spectrometer with a Zspray™ electrospray ionization (ESI) source. Data acquisition was done using the Waters MassLynx software.

Mass spectrometry (MS) analyses were conducted in *electrospray* positive mode (ESI +) employing the multiple reaction monitoring (MRM) mode, with two transitions being used for qualitative and quantitative identification of the studied analytes. Detailed information on the monitored MRM transitions of the antibiotics and pesticides is presented in Table 2**.** For LC analysis, experiments were conducted at 35 °C with an injection volume of 1 µL. A gradient elution method was employed using mobile phases A (water) acidified with 0.1 % formic

Table 2
MRM parameters for the ESI (+) analysis of the pesticides and antibiotics.

Analyte	Precursor	M1 Quantitative	CV	CE	M2 Qualitative	CV	CE
PESTICIDES							
Atrazine	216.0	132.0	34	20	174.0	30	20
Thiamethoxam	292.0	211.0	25	10	181.0	40	20
ANTIBIOTICS							
Sulfanilamide	173.0	92.0	30	17	156.0	10	7
Ceftiofur	524.0	241.0	35	16	125.0	20	30

M1: First monitored ion; **M2:** Second monitored ion; **CV:** Cone voltage; **CE:** Collision energy.

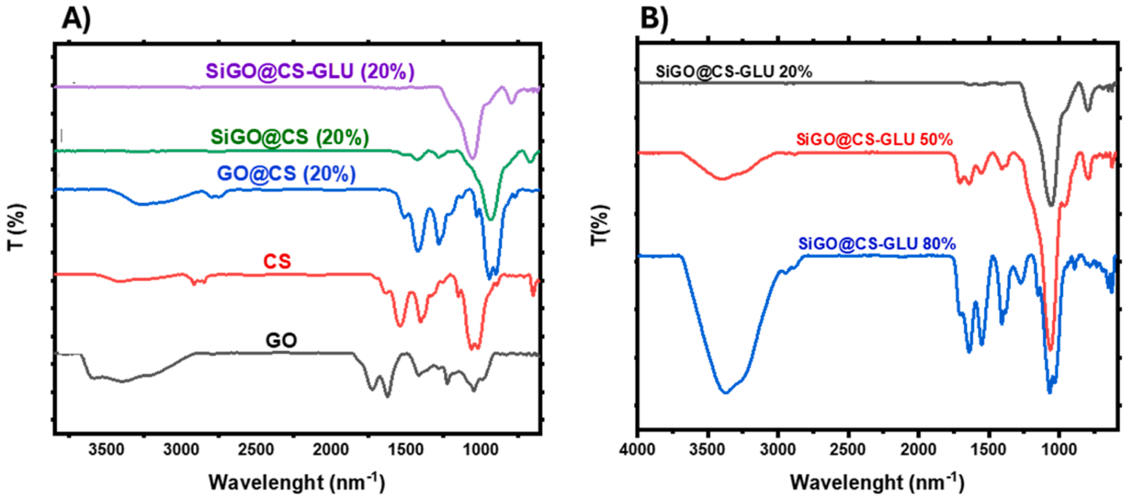

Fig. 1. FTIR spectra of the **(A)** GO, CS aerogel, GO@CS 20 %, SiGO@CS 20 %, SiGO@CS-GLU 20 %, and **(B)** SiGO@CS-GLU at different percentages of CS/SiGO (w/w).

acid and B (ACN) at a flow rate of 6 μL min^{-1}. The LC gradient began with 20 % B, increasing to 60 % B over 6 min. This condition was maintained until 8 min, after which the percentage of B was returned to the initial 20 %. The initial condition was held constant from 9 to 13 min to re-equilibrate the column for the next injection, resulting in a total LC-MS/MS analysis time of 13 min.

2.8. *Figures of merits*

The evaluation of key performance metrics for the developed MEPS LC-MS/MS method, including linearity, recovery, intermediate precision, repeatability, limit of quantification (LOQ), and limit of detection (LOD), was conducted following the validation guidelines of the International Conference on Harmonization (ICH) [30]. The spiked solutions described in Section 2.6 were used to evaluate these parameters. Linearity was assessed by determining the coefficient of determination (R^2) from analytical curves generated through linear regression of the pesticide peak areas (Y) against the pesticide concentrations (X, μg L^{-1}) across seven concentration levels, ranging from 10 to 500 μg l^{-1} ($n = 3$). The LOD and LOQ were established by comparing the signal of the chromatograms from the spiked sample to the noise from the blank sample. Therefore, the LOD was defined as the concentration at which a signal-to-noise ratio of 3:1 was achieved, while for the LOQ, a signal-to-noise ratio of 10:1 was used as the criterion. Moreover, trueness and precision were evaluated at three concentration levels from the analytical curve, corresponding to high (400 μg L^{-1}), medium (200 μg L^{-1}), and low (50 μg L^{-1}) levels, with three replicates for each level ($n = 3$). These assessments were conducted over three days to determine intra-day and inter-day variation coefficients (CV%). For evaluating the matrix effect (ME), the matrix-matched calibration (MMC) method was utilized [31]. Analytical curves for the target analytes were constructed in both ultra-purified water and food matrices across six concentration levels (10 to 500 μg L^{-1}). Each assay was performed in triplicate ($n = 3$). Therefore, the matrix effect was discussed regarding signal suppression or intensification (SSE), as described in Eq. (1).

$$\mathrm{SSE} = \left(1 - \frac{\mathrm{SM}}{\mathrm{SS}}\right) x\ 100 \tag{1}$$

SM represents the slope of the analytical curve obtained in the matrix, and **SS** represents the slope of the analytical curve in the solvent.

3. Results and discussion

3.1. *Characterization of the SiGO@CS biosorbent*

Before the MEPS application, the biosorbents synthesized in Section 2.3 underwent characterization assays to evaluate their differences and verify the success of the modifications in alignment with the initial objectives. Fig. 1**A** presents the FTIR spectra obtained for the sorbent: GO, pure CS, GO/CS, SiGO@CS-GLU, and SiGO@CS with no glutaraldehyde. Following the sequence in Fig. 1**A**, the GO spectra exhibit distinct peaks from various oxygen-containing functional groups. The vibration observed at 3267 cm^{-1} corresponds to the O-H stretching bond from hydroxyl groups within the GO structure. Additionally, the band at 1712 cm^{-1} is attributed to carboxyl groups. Adjacent to the peak at 1712 cm^{-1}, the peak at 1618 cm^{-1} was considered to result from the stretching and bending vibrations of O-H functional groups from water molecules in the GO composition. The 1402 cm^{-1} and 1220 cm^{-1} peaks are assigned to C-OH and C-O-C stretching, respectively. Finally, the peak at 1012 cm^{-1} is attributed to the vibrational mode of the C-O group. The obtained spectra for GO were based on previous observations from our reported studies [23,24].

The pure CS aerogel obtained without adding GO provided valuable information that was used later to discuss the characterization of the

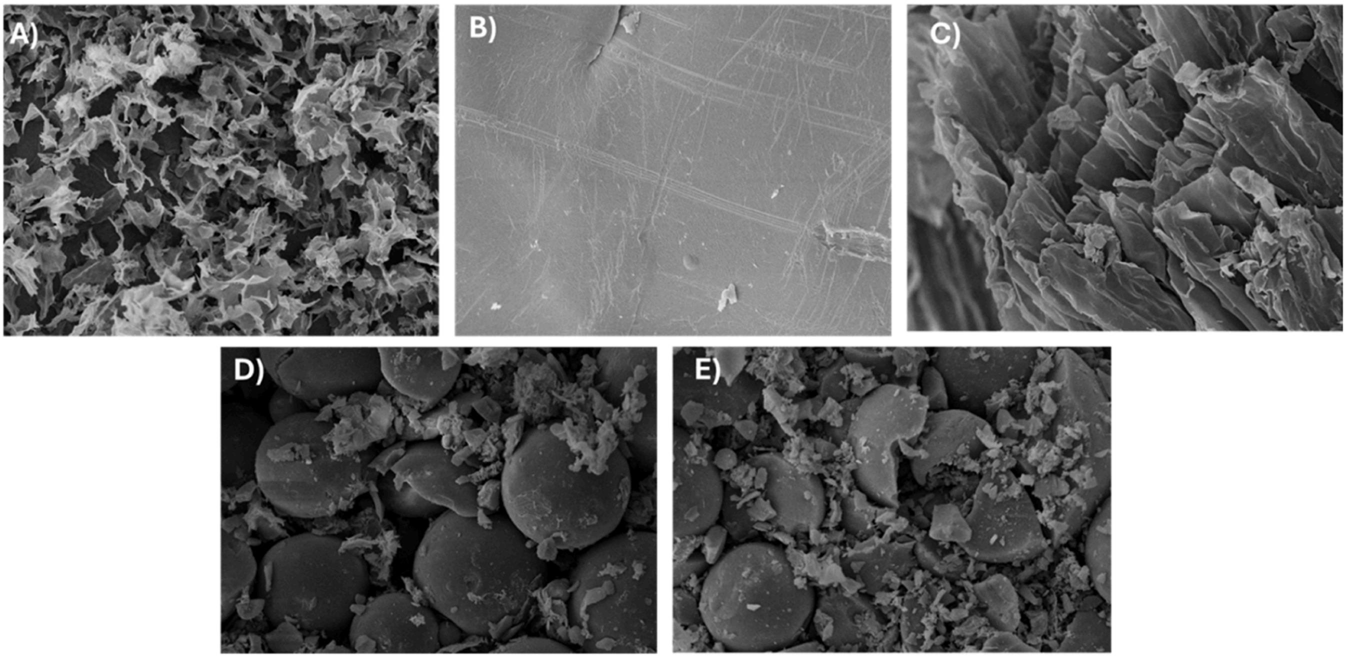

Fig. 2. SEM images of the synthesized materials: **(A)** GO, **(B)** pure CS aerogel, **(C)** GO@CS, **(D)** SiGO@CS, and **(E)** SiGO@CS-GLU at 2000x magnification.

synthesized materials. According to Fig. 1**A**, the spectra of the CS aerogel show a peak at 3423 cm^{-1}, attributed to the abundant O-H and N-H stretching vibration from the hydroxyl and amino groups. According to Shi et al. [32] bands at 2910 and 2852 cm^{-1} can be attributed to the stretching vibration of C-H. Additionally, the peaks observed at 1631, 1525, and 1400 cm^{-1} correspond to the C=O stretching of amide (amide I), the N-H bending of –NH_2 (amide II), and C-NH_2 respectively [33]. Moreover, the peaks in the range of 900–1031 cm^{-1} are associated with C-O-C and C-O-H stretching, while 889 cm^{-1} is described as the stretching of the pyranose ring [34]. As expected, the spectra of GO@CS (Fig. 1**A**) exhibit characteristics from both GO and CS. According to the literature, GO@CS composites are primarily formed through reactions between the GO surface's epoxy groups and the CS surface's amino groups.

Additionally, the covalent bonding created during the crosslinking between GO and CS helps retard the decomposition of the amine units in CS [33,35]. Although the resulting spectra show some similarities to those of the starting materials, there are also notable differences. For instance, the peak at 1741 cm^{-1}, present in GO, is absent in the GO@CS polymer. Peng et al. [36] attribute the disappearance of this peak to the reaction between the carboxyl groups of GO and the amino or hydroxyl groups of CS.

As previously mentioned, using G-based materials in microextraction procedures, such as MEPS, can cause a backpressure effect [17,18]. However, modifying GO@CS with Si was evaluated in this study as a solution to this challenge. Interestingly, the final FTIR spectra of SiGO@CS (Fig. 1**A**) showed more remarkable similarity to the CS than the GO spectra. For example, peaks at 1525 cm^{-1}, 1424 cm^{-1}, and 1284 cm^{-1} correspond to the C=O stretching of amide (amide I), the N-H bending of –NH_2 (amide II), and C-NH_2, respectively, which are characteristic of the CS aerogel. The intense peak at 933 cm^{-1} is also attributed to the overlapping of Si-O-Si and the C-O-C from the glycosidic linkage [37].

Although the synthesis of a SiGO@CS biosorbent could mitigate the backpressure challenge in MEPS applications, experimental assays demonstrated that the non-linked CS in the biopolymer restricted the passage of the sample solution through the frits in the BIN compartment. To address this issue, this study proposed using a 25 % glutaraldehyde solution in H_2O to ensure maximum crosslinking through covalent bonds between SiGO and CS during the synthesis reaction. Moreover, the literature supports the use of glutaraldehyde as an effective method for enhancing the stability of polysaccharides. in an aqueous environment, even with the presence of GO [34]. As illustrated in Fig. 1**A,** no visual differences were observed in the obtained FTIR spectra of SiGO@CS-GLU compared to the one without adding the glutaraldehyde solution, both with 20 % of CS/SiGO (w/w).

As reported in Section 2.3, different SiGO@CS-GLU biosorbents were synthesized with varying percentages (20 %, 50 %, and 80 %) of CS/SiGO (w/w) to identify the primary differences between the materials. The varying percentage of CS to GO was anticipated to produce distinct FTIR spectra for the materials. As shown in Fig. 1**B**, the SiGO@CS-GLU sorbent with 20 % CS to GO displayed spectra lacking characteristic CS peaks. Specifically, the typical peaks at 3000–3600 cm^{-1} and at 1630, 1525, and 1400 cm^{-1}, which correspond to the C=O stretching of amide (amide I), the N-H bending of –NH_2 (amide II), and C-NH_2, respectively, were not observed [33]. On the other hand, increasing the proportion of CS in the SiGO@CS-GLU biosorbent resulted in spectra that more closely resembled the profile of pure CS. The biosorbent with 80 % CS to GO (w/w) exhibited higher transmittance (T%) values, attributable to the more significant presence of CS during synthesis (Fig. 1**B**).

SEM analyses were conducted to gain deeper insights into the morphological characteristics of the developed materials. The SEM surface images obtained from these analyses are displayed in Fig. 2. Fig. 2**A** shows a representative SEM image of the GO materials, revealing their characteristic 2D nanosheet morphology [38]. A detailed examination of the GO surface shows the presence of wrinkled and folded textures, typical features of GO. These morphological characteristics confirm the successful attachment of oxygen-containing functional groups, indicating the successful synthesis of the material [39]. The evaluation of pure CS aerogel, as shown in Fig. 2**B**, reveals a distinct surface morphology compared to GO. The SEM images depict a CS sheet-like configuration with a smooth and regular surface at a magnification of 2000x. These observations are consistent with those reported in the literature [40]. An insightful observation was made upon analyzing Fig. 2**C**, which presents the SEM image of the GO@CS biosorbent. Integrating GO and CS resulted in a highly porous and interconnected 3D network structure. According to Gong et al. [41], the incorporation of GO induces a lamellar configuration in the final

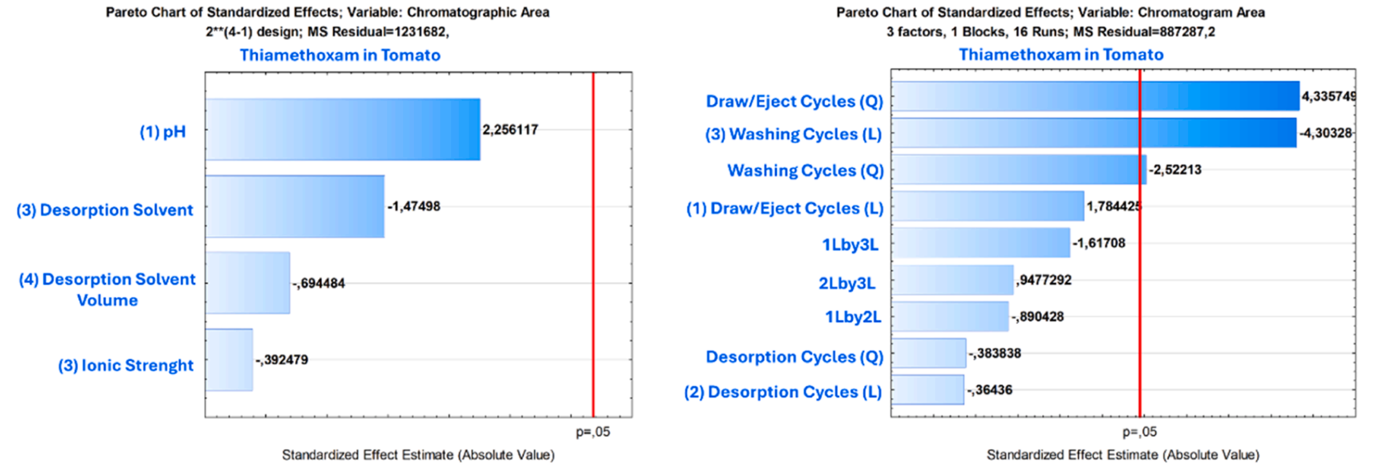

Fig. 3. Obtained results for the MEPS optimization of thiamethoxam extraction in tomato samples: **(A)** Pareto chart of 2^{4-1} and **(B)** Pareto chart of 2^3.

structure, underscoring the substantial influence of GO on the morphological properties of the GO@CS composite material.

The introduction of Si to create the SiGO@CS composite material resulted in a distinctive morphological structure. As illustrated in Fig. 2**D**, well-defined Si microspheres were evident. A closer examination reveals the presence of nanostructures in the form of nanosheets on the Si surface, indicating the successful modification of Si with GO and CS. A comparable surface appearance was observed for the SiGO@CS-GLU biosorbent. Figs. 2**D** and 2**E** reveal intriguing insights into the biosorbents SiGO@CS and SiGO@CS-GLU (with 20 % of CS/GO w/w). Despite their similarities, the biosorbent synthesized with the addition of glutaraldehyde solution exhibited a visibly higher abundance of nanosheets on its surface, indicating superior modification by this strategy. This enhanced visualization is evident in the SEM images at 500x magnification shown in **Fig. S2.**

EDX analyses were employed to determine the elemental composition of the developed sorbents. The spectrum for the synthesized materials revealed a high content of carbon and oxygen in the GO-based materials. The biosorbents synthesized with CS also showed a significant presence of nitrogen, attributed to the amino and acetamido groups, as demonstrated in the FTIR spectra (Fig. 1**A**). Moreover, the obtained SiGO@CS and SiGO@CS-GLU polymers exhibited a high content of Si, along with other elements inherent to the chemical structures of GO and CS. As expected, increasing the CS content in the SiGO@CS-GLU biosorbents resulted in a higher nitrogen abundance. The biosorbent with the highest CS content (80 %) demonstrated the most significant nitrogen presence compared to the others. Detailed elemental percentage information obtained from EDX spectra is presented in **Fig. S3**.

3.2. MEPS optimization

Two experimental designs were implemented for a better understanding of the MEPS extraction efficiency for the analyzed compounds. The initial design utilized a 2^{4-1} fractional factorial design to assess the effects of sample pH, ionic strength (NaCl concentration, w/v%), desorption solvent type, and desorption solvent volume. These factors were prioritized due to their substantial impact on the overall MEPS performance. Given the nature of the study, which encompassed analytes with diverse physicochemical properties (as detailed in **Table S1**), the optimal extraction conditions were determined based on the experimental outcomes.

Fig. 3**A** outlines the main parameters evaluated in the 2^{4-1} fractional factorial design and their influence on MEPS extraction performance for the evaluation of THI in tomato samples. While the statistical analysis depicted in Fig. 3**A** indicates that the evaluated parameters had no significant impact, it is noteworthy that for the extraction of THI in tomato, the pH and desorption solvent were the most influential parameters. Conversely, for the extraction of ATR in corn samples, neither visual inspection nor statistical analysis revealed significant influences of pH, ionic strength, desorption solvent type, or desorption solvent volume on the MEPS extraction performance. The optimal parameters for extracting THI and ATR in corn and tomato samples were determined by combining pareto chart information and the area under each chromatographic peak (**Figs. S4 and S5**). Consequently, the MEPS extraction of THI and ATR was optimized using a sample pH of 7 and 100 μL of ACN as the desorption solvent and no salt added (w/v of NaCl). No statistically significant influences were observed when extracting CEF and SUL in the milk samples. However, among the evaluated parameters, the desorption solvent emerged as the second most influential factor for both analytes.

Moreover, the most influential parameter for both analytes was found to be the ionic strength. Adding 20 % NaCl (w/v) harmed MEPS extraction efficiency for SUL extraction, according to the 2^{4-1} fractional factorial design. On the other hand, the evaluation of the MEPS extraction efficiency demonstrated that the extraction of CEF in milk was enhanced by adding 20 % NaCl (w/v). The optimal extraction conditions were determined by combining Pareto chart information with the area under each chromatographic peak. The study chose the best extraction conditions without adding salt to enable the simultaneous extraction of SUL and CEF. As shown in **Fig. S4**, the chromatographic area peak for CEF was superior to that of SUL. Therefore, to ensure adequate extraction of SUL, the final method excluded the addition of salt due to its negative effect on the MEPS extraction of SUL. Additionally, the best extraction condition for both analytes in milk was considered using a sample pH of 7 and 100 μL of MeCN as the desorption solvent. Detailed information on the 2^{4-1} fractional factorial design and the chromatography peak area can be found in the supplementary material (**Figs. S4 and S5**).

Following the MEPS optimization, the sampling, washing, and elution cycle parameters were evaluated using a full factorial design 2^3 with three central points. Fig. 3 illustrates that the draw/eject and washing cycles were the most influential parameters for THI extraction in tomato samples. The results suggested that increasing the sampling cycles until the central point positively affects THI extraction while increasing the washing cycles negatively influences it. For the MEPS extraction of ATR, the washing cycles emerged as the most influential parameter, as shown in **Fig. S5** The statistical evaluation using the Pareto chart for the 2^3 design in extracting CEF from milk samples revealed no significant influence from the sampling, washing, and elution cycles during the MEPS procedure (**Fig. S5**). However, for the MEPS optimization of SUL extraction, the washing cycles emerged as the most influential parameter, indicating that increasing the washing

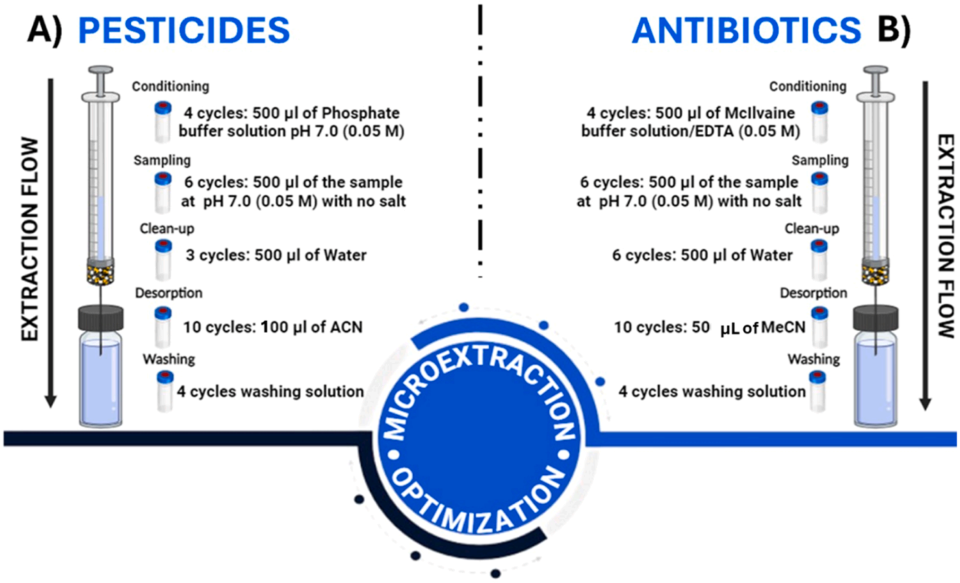

Fig. 4. MEPS optimum conditions for the extraction of **(A)** Thiamethoxam and Atrazine in corn and tomato samples and **(B)** Sulfonamide and Ceftiofur in milk samples.

cycles negatively impacted the extraction efficiency (**Fig. S5**).

A final evaluation using a desirability function identified the optimal conditions for each parameter in the 2^3 factorial design. This evaluation indicated that an intermediary condition was the best option for MEPS extraction of THI and ATR in tomato and corn samples. Consequently, the optimal extraction conditions for these analytes were determined to be 6 sampling cycles, 3 washing cycles, and 10 desorption cycles. A similar optimal condition was identified for the MEPS extraction of CEF and SUL in milk samples, and more washing cycles were performed than for the pesticides. In this case, 6 sampling and 10 desorption cycles were adequate, along with 6 washing cycles, providing better extraction conditions. Fig. 4 illustrates the best MEPS extraction condition for the studies of pesticides (Fig. 4**A**) and antibiotics (Fig. 4**B**) in their respective food matrices according to the optimization study conducted by the 2^{4-1} and 2^3 evaluation.

3.3. Extraction performance of the synthesized biosorbents and their comparison with traditional sorbent-packed phases

As detailed in *Section 2.3*, this study proposed the synthesis of different SiGO@CS-GLU biosorbents with differing CS/SiGO w/w percentages (20 %, 50 %, and 80 %). To assess the impact of these percentages on extraction efficiency in the MEPS procedure, the polymers were tested for their ability to extract pesticides from corn and tomato and antibiotics from milk (both at 100 µg L^{-1}) samples. Moreover, the extraction efficiency of these biosorbents was compared to traditional sorbent phases commonly used in solid-based extraction methods. Specifically, Si and NH_2 sorbents were evaluated using the same MEPS protocol outlined in Fig. 4 to extract pesticides and antibiotics from food matrices. The results of this assessment are presented in **Fig. S6** as the average chromatographic area for the pesticides and antibiotics.

As detailed in **Fig. S6**, a clear trend is observed when comparing the chromatographic areas obtained for pesticides and antibiotics at the same concentration (100 µg L^{-1}). The results indicate a higher efficiency of the biosorbents for applications in corn and tomato samples, highlighting the increased complexity of animal-origin food matrices. Furthermore, more interpretations concerning the extraction efficiency of the sorbent can be taken from **Fig. S6**. According to the findings, increasing the percentage of CS in the polymer enhances the extraction performance of the SiGO@CS-GLU biosorbent. Specifically, the biosorbent synthesized with 80 % CS/SiGO w/w exhibited the best extraction efficiency compared with biosorbents with lower CS percentages, highlighting the positive impact of CS presence in the final material. This improvement is particularly evident when comparing the biosorbents' performance to unmodified SiGO. Moreover, the 50 % and 80 % CS/SiGO w/w biosorbents demonstrated superior extraction efficiency compared to pure SiGO sorbent.

To the author's knowledge, this was the first time the proposed SiGO@CS-GLU biosorbent was applied in a MEPS protocol for extracting pesticides and antibiotics from food samples. Consequently, it is challenging to find comparable studies to evaluate the extraction behavior observed in this study based on the percentage of CS/SiGO w/w and the comparison with traditional sorbent phases. However, a study by Wu et al. [42] presented the synthesis of three-dimensional chitosan-grafted graphene oxide aerogels modified with silica (3D CS/GOA@Sil) using a distinct protocol from that employed in our study for conventional solid-phase extraction (SPE) of herbicides in vegetables. Their comparison with traditional SPE sorbents, including NH_2, demonstrated the superior efficiency of the 3D CS/GOA@Sil sorbent. The authors noted that incorporating chitosan reduced the aggregation of graphene oxide sheets, thereby enhancing the extraction efficiency of herbicides in food samples. Similar findings were observed in our study, where the SiGO@CS-GLU 80 % biosorbent exhibited superior extraction efficiency for both pesticides and antibiotics compared to SiO_2 and NH_2 sorbents, particularly in the extraction of antibiotics compared to the NH_2 sorbent.

Furthermore, the literature highlights the remarkable adsorption capabilities of GO-based materials due to their high surface area, which provides suitable conditions for the adsorption of target analytes [43, 44]. Therefore, based on the main findings, we can infer that adding and increasing amounts of CS in the sorbent enhances the biosorbent's activity toward pesticides and antibiotics. This enhanced selectivity is likely linked to the potential interactions between the target analytes and the functional groups present in the CS chemical structure, such as -OH and -NH_2, facilitating chemical interactions, such as hydrogen bonding and π-π interaction with the target analytes [19]. Moreover, combined with the stabilizing effect of the GO nanosheets that the addition of CS has to the final SiGO@CS-GLU 80 % sorbent significantly improves its application as packed sorbent for the MEPS extraction of pesticides and antibiotics in food samples.

Table 3
Obtained figures of merits using MMC lines for the extraction of pesticides and antibiotics in food samples through the MEPS LC-MS/MS method.

Compound	Regression Equation	R^2	Range (μg L^{-1})	LOQ (μg L^{-1})	LOD (μg L^{-1})	Spiking Level (μg L^{-1})	Trueness (%)	Precision RSD (%)		
								Day 1	Day 2	Day 3
ATR	41.242x + 44,753.2	0.9909	10–500	0.045		50	100	9	2	3
					0.020	200	90	8	11	4
						400	96	8	9	3
THI	11.594x + 770.1	0.9980	10–500	1.0		50	92	12	4	5
					0.045	200	109	11	2	6
						400	105	14	4	12
CEF	3.486x + 1001.3	0.9952	25–500	15		50	89	2	5	13
					5	200	107	9	3	6
						400	87	10	15	7
SUL	0.331x + 163.1	0.9912	25–500			50	82	4	5	5
				20	15	200	104	5	8	8
						400	84	7	2	2

3.4. Figures of merits

The figures of merit in this study involved a thorough evaluation of multiple analytical parameters, following the validation guidelines set by the ICH, to confirm the method's applicability. Linearity was assessed by constructing analytical curves in the matrix over a concentration range of 10 to 500 μg L^{-1} ($n = 3$). The results indicated that the method exhibited excellent linearity for pesticides and antibiotics in food matrices, with correlation coefficients (R^2) more significant than 0.9900 for all analytes. Moreover, intra and inter-day precision were evaluated as the relative standard deviation (RSD%) response. Intra-day precision (day 1) values ranged from 2 to 14 %, while inter-day precision (day 1, 2, and 3) values ranged from 2 to 15 %. Trueness was assessed at three concentration levels: low (50 μg l^{-1}), medium (200 μg l^{-1}), and high (400 μg l^{-1}). The reported MEPS LC-MS/MS method achieved values ranging from 82 % to 109 % for trueness assays. Furthermore, the LOD and LOQ values for pesticides in corn and tomato ranged from 0.020 to 1.0 μg l^{-1}. Regarding the evaluation of antibiotics in milk, LOD and LOQ values ranged from 5 to 20 μg l^{-1}. Detailed information corresponding to the figures of merits using MMC lines for each analyte in food matrices is presented in Table 3.

The ME assessment of the method can elucidate the true impact of the matrix presence on the suppression or enhancement of the analytical signal for each analyte [45]. To evaluate this influence, the MMC strategy was employed to determine the effect of the evaluated food samples on the analytical response to pesticides and antibiotics. Based on **Eq. (1)**, the calculated MMC values indicated a suppression effect of the matrix on the analytical signal for the pesticides ATR and THI, with suppression levels of 6 % in corn and 37 % in tomato, respectively. A similar suppression effect was observed for the antibiotic CEF, with an 84 % reduction in signal. Conversely, the matrix positively impacted the analytical signal for SUL in milk, enhancing the analytical signal by 73 %. The application of the MMC method demonstrated that the matrix effect significantly impacted the analytical response (chromatographic peak area) of the studied analytes in food matrices, highlighting its critical consideration. Despite the observed ME, this study proposed optimization and validation of the MEPS protocol in the matrix, effectively compensating for these effects and providing a more real analytical scenario of the reported MEPS LC-MS/MS approach for antibiotics and pesticides in food matrices. Moreover, a representative chromatogram (50 μg L^{-1}) of the monitored quantified MRM transitions (Table 2) for the evaluated pesticides and antibiotics is presented in **Fig. S7**.

In a microextraction protocol, achieving low values of LOD and LOQ is highly expected. This aligns with the main principle of MEPS strategies, where the use of packed sorbent in the MEPS syringe enables the preconcentration of trace-level concentrations. Applying the adequate MEPS approach allows for a realistic evaluation of these low concentrations in complex matrices, such as food samples. Moreover, the analytical performance of the method is primarily linked to the capability of the sorbent to offer optimal extraction conditions. The reported SiGO@CS-GLU 80 % provided remarkable analytical performance, as demonstrated by the figures of merit in this section. The developed biosorbent's application enhanced MEPS extraction by achieving low LOD and LOQ values for antibiotics and pesticides. It maintained its analytical performance over 15 reuses, with an RSD% of <15 %. Besides, the MEPS procedure took around 5 min (steps presented in Fig. 4), demonstrating a considerable analytical throughput. The developed MEPS LC-MS/MS method using SiGO@CS-GLU 80 % as the packed sorbent shows excellent potential for monitoring ATR, THI, CEF, and SUL in corn, tomato, and milk samples.

3.5. Application of the MEPS LC-MS/MS method in local market food samples

As detailed in Section 2.5, this study applied the MEPS LC-MS/MS method to evaluate ATR and THI in corn and tomato samples and CEF and SUL in milk matrices, following the extraction steps specified in Fig. 4. Food samples were collected from different São Paulo, Brazil regions and subjected to the MEPS extraction method using the SiGO@CS-GLU 80 % biosorbent. Therefore, 3 samples of tomato and corn were obtained, while two samples were used for milk evaluation. According to the main results, the pesticide THI was detected lower than the LOQ value in two tomato samples, while one sample presented a quantified concentration of 139.0 μg l^{-1}. The obtained THI concentration in the tomato sample was found to be higher than the maximum concentration of ingestion per day allowed by Agência Nacional de Vigilância Sanitária (ANVISA) in Brazil (20 μg l^{-1}) [46] and the maximum limits of residue (MLR) established by the European Food Safety Authority (EFSA) (10 μg l^{-1}) [47].

Moreover, out of the three corn samples evaluated, only one showed a quantified concentration, which was found to be 221.6 μg l^{-1}. This concentration exceeds the MRL established by the EFSA, which is 50 μg l^{-1} [47]. Furthermore, according to ANVISA, although the maximum concentration allowable of ATR in corn samples is 250 μg l^{-1}, daily pesticide consumption should not exceed 20 μg l^{-1}, as specified by the legislation [46]. In the milk sample analysis, only CEF was detected below the LOQ values established in this study (15 μg l^{-1} for CEF and 20 μg l^{-1} for SUL). These findings are consistent with ANVISA and EFSA regulations, which permit an MRL concentration of 100 μg l^{-1} for both antibiotics in milk samples [46,47].

As demonstrated, the developed SiGO@CS-GLU 80 % used in the MEPS extraction approach is an adequate analytical strategy to detect and quantify pesticide concentrations exceeding the regulatory limits for THI and ATR in one of the three tomato and corn samples evaluated. These findings highlight the effectiveness of our MEPS LC-MS/MS method in evaluating pesticides in food samples. Although no quantifiable concentrations of antibiotics were found, the method provided adequate analytical conditions for their detection and potential

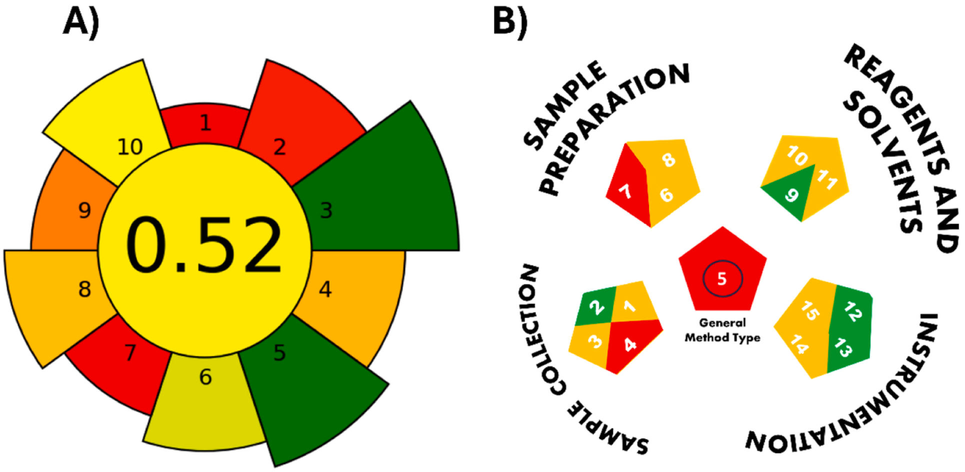

Fig. 5. Green analytical evaluation of the developed MEPS method by using **(A)** AGREEprep and **(B)** GAPI indicators.

quantification, supporting its application in milk samples.

3.6. Literature comparison and green aspects assessment of the MEPS LC-MS/MS method

One of the primary advantages of miniaturized extraction protocols is their environmental friendliness compared to traditional methods. Therefore, these microextraction strategies are anticipated to leverage the fundamental principles of GAC to propose new eco-friendly analytical approaches for evaluating complex matrices, such as food samples. Different approaches are reported in the literature to introduce new metrics encompassing critical considerations for distinguishing eco-friendly analytical assessments from traditional methods. This study proposes applying the AGREEprep tool to evaluate the ten principles established by green sample preparation (GSP) and the green analytical procedure index (GAPI). The AGREE score and the GAPI diagram obtained for the MEPS LC-MS/MS evaluation are presented in Fig. 5 as follows.

Detailed information on the values and data used in both evaluations is provided in **Tables S2** and **S3** in the supplementary material. As depicted in Fig. 5 and information in the supplementary material, a consistent finding between these evaluations was the detrimental impact observed on the performance of offline analysis in both strategies. Offline methodologies can increase the number of steps, leading to substantial solvent consumption and reduced analytical throughput. In line with this, the reported MEPS LC-MS/MS method still involves a considerable number of steps starting from extract preparation, including the use of 5 mL of acetonitrile and the energy consumption for drying the samples, which, as indicated by the software, requires careful evaluation. However, using MEPS as the extraction protocol helps mitigate this drawback, as only a few microliters of the pre-treated sample extract are needed for the extraction. Consequently, the initial extraction steps are performed only once, as the final volume is sufficient for performing several MEPS extractions. This significantly reduces the environmental impact compared to conventional sample preparation methods.

Despite the pointed disadvantages, the proposed study promoted the remarkable use of just 5 min of the MEPS steps, thus leading to the possibility of performing >10 extractions per hour, which is highly desirable to an offline extraction protocol. Although the MEPS method evaluation was affected in AGREEprep and GAPI assessments due to its extraction type, initial solvent consumption, and the number of performed steps Fig. 5 highlighted its green analytical aspects. These included the utilization of the SiGO@CS-GLU biosorbent, which is notable for its reusability (>15 times). Impregnating biosorbents enhances methodological green metrics, as these materials are typically biodegradable and synthesized under less harmful conditions for humans [48]. Additionally, intrinsic features of the microextraction method, such as using a low pre-treated sample extract volume (500 μL), further promoted environmentally friendly analytical conditions.

The versatility of microextraction methods has been demonstrated across various applications, including the evaluation of contaminants in food matrices, such as pesticides and antibiotics. As reported in the literature, these applications provide relevant benchmarks for comparing with the MEPS LC-MS/MS method described in this study. By highlighting key aspects, we underscore the superior applicability of our method over other microextraction protocols for assessing pesticides and antibiotics in food matrices. In this context, Andrade et al. [49]. reported using bar adsorptive microextraction (BAμE) coated with a molecularly imprinted polymer (MIP) for the extraction of triazines in corn samples. The authors achieved optimal extraction conditions with a 60 min extraction time, enabling one per hour. The method demonstrated a LOD of 0.2 μg l^{-1} and recovery values ranging from 81 % to 119 %. In contrast, our proposal achieved an extraction time of just 5 min, allowing 12 extractions per hour with a superior LOD for ATR in corn samples (0.020 μg l^{-1}).

While analytical parameters are crucial for evaluating the applicability of a method, it is equally important to consider its environmental impact, especially when using microextraction protocols. Recently, Abbasalizadeh et al. [50]. combined dispersive solid-phase extraction with dispersive liquid-liquid microextraction (DSPE-DLLME) using a carbon-based sorbent to assess organophosphorus pesticides in vegetable samples, including tomatoes. Their extraction procedure used 5 mL of pre-treated sample extract volume and 10 mg of sorbent. In contrast, our study used only 500 μL of pre-treated sample extract volume and 7 mg of sorbent. Despite the seemingly minor difference in sorbent mass, 500 μL of sample significantly reduces chemical waste. This reduction is significant during method development, which requires numerous extractions and consequently generates substantial chemical waste.

Dispersive liquid-liquid microextraction (DDLME) using hydrophobic deep eutectic solvents (hDESs) as green extractants was utilized for assessing antibiotics in milk samples by Sereshti et al. [51]. The authors reported LOD values ranging from 5.1 to 28.4 μg L^{-1} using a 7 mL sample volume containing the selected antibiotics. In our MEPS LC-MS/MS study, we extracted antibiotics using 500 μL of pre-treated sample extract volume, allowing us to perform 14 extractions with the same volume used by Sereshti et al. Moreover, our study obtained superior LOD values for CEF and SUL evaluation in milk matrices (5–15 μg L^{-1}). This demonstrates that our method offers a potential and alternative approach to other microextraction strategies for assessing pesticides and antibiotics in food samples.

The notable advantages of our developed method include achieving

Table 4

Comparison of literature on the microextraction of pesticides and antibiotics in food samples.

Analyte(s)	Sample	Analytical Technique	Sample Volume (mL)	Extraction Time (min)	LOD μg L^{-1}	Refs.
Triazines	Corn	BAμE(MIP)- μLD–LC–DAD	25	60	0.2	[49]
Carbamate pesticides	Corn	SBSE-HPLC-VWD	10	50	0.017–0.048	[52]
Organophosphorus pesticides	Vegetables (Including tomato)	DSPE-DLLME-GC-FID	5	5	0.2	[50]
Pesticides	Tomato	MDSPE-DLLME-GC–MS	10	0.5	0.06–0.33	[53]
Antibiotics	Milk	hDES-based DLLME-LC-UV	7	–	5.1 to 28.4	[51]
Antibiotics	Milk	DLLME-LC-DAD	7	20	2.0–2.8	[54]
Pesticides and Antibiotics	Corn, tomato, and milk	MEPS LC-MS/MS	0.5	5	0.020–5.0	**This Study**

BAμE(MIP)- μLD–LC–DAD: Bar adsorptive microextraction coated with a selective molecularly imprinted polymer micro-liquid desorption followed by diode array detection; **DSPE-DLLME-GC-FID:** Dispersive solid-phase extraction with dispersive liquid-liquid microextraction- gas chromatography-flame ionization detector; **hDES-based DLLME-LC-UV:** Hydrophobic deep eutectic solvents dispersive liquid-liquid microextraction-liquid chromatography with ultraviolet-vis detection; **DLLME-LC-DAD:** Dispersive liquid-liquid microextraction- liquid chromatography with diode-array detection; **SBSE-LC-VWD:** Stir-bar solvent extraction- liquid chromatography-variable wavelength ultraviolet detector**;** **MDSPE-DLLME-GC–MS:** Magnetic solid phase extraction- dispersive liquid-liquid microextraction- gas chromatography-mass spectrometry; **MEPS LC-MS/MS:** Microextraction by packed sorbent coupled with liquid chromatography-tandem mass spectrometry;.

low LOD and LOQ values and adequate trueness results. These analytical parameters are crucial for detecting and quantifying trace-level concentrations of these chemicals in food matrices. Additionally, the remarkable reusability of our developed phase (>15 times) highlights the potential of our biosorbent over traditional sorbent phases, presenting a low-cost and eco-friendly strategy aligned with microextraction protocols, particularly for MEPS strategies. Table 4 presents some literature reports on microextraction strategies that evaluate pesticides in food matrices. It's important to highlight that Table 4 provides information specifically about the microextraction protocol rather than the complete analytical method.

4. Conclusions

This study presented a novel biosorbent combining SiGO and CS for the MEPS extraction of pesticides and antibiotics from food matrices. Characterization assays confirmed the successful modification of SiGO particles with CS, identifying the sorbent with the highest CS content (80 %) as the most effective option for the MEPS protocol targeting the selected analytes. The optimization of the MEPS LC-MS/MS method highlighted the draw/eject and washing cycles as the most influential parameters affecting extraction efficiency. The figures of merit obtained using MMC lines to correct the observed ME demonstrated excellent sensitivity, with R^2 values greater than 0.9900. The LOD ranged from 0.020 to 0.045 μg L^{-1} for pesticides and 5 to 15 μg L^{-1} for antibiotics, while the LOQ were between 0.045 and 1.0 μg L^{-1} for pesticides and 15 to 20 μg L^{-1} for antibiotics. Trueness values were between 82 % and 109 %, indicating the robust performance of the method.

Comparison studies of the biosorbent with traditional non-modified SiGO and other sorbents (Si and NH_2) demonstrated the superior performance of the SiGO@CS-GLU 80 % biosorbent. Furthermore, the application of this biosorbent in the MEPS LC-MS/MS protocol enabled the detection and quantification of elevated pesticide levels in corn and tomato matrices, using a methodology that required only 5 min of the microextraction protocol, a minimal pre-treated sample extract volume (500 μL), and allowed the reuse of the sorbent for over 15 extractions. The reported MEPS LC-MS/MS method using the proposed SiGO@CS-GLU 80 % biosorbent proved to be a valuable tool for detecting pesticides and antibiotics and identifying permissible or elevated concentrations in food matrices, incorporating eco-friendly aspects in line with green analytical practices.

CRediT authorship contribution statement

Rafael O. Martins: Writing – review & editing, Writing – original draft, Methodology, Investigation, Data curation, Conceptualization. **Fernando M. Lanças:** Writing – review & editing, Writing – original draft, Supervision, Project administration, Funding acquisition, Conceptualization.

Declaration of competing interest

The authors affirm that they have no identifiable competing financial interests or personal relationships that might have influenced the research reported in this paper.

Acknowledgments

The São Paulo Research Foundation, FAPESP [Grants 2017/02147–0; 2017/21984–0 – EMU; 2017/21985–6 – EMU; 2023/15675–5 and 2023/07159–7]; and the National Council for Scientific and Technological Development, CNPq [Grants 308843/ 2019–3 and INCT-ALIM Grant 406760/2022–5] supported this work.

Supplementary materials

Supplementary material associated with this article can be found, in the online version, at doi:10.1016/j.sampre.2024.100134.

Data availability

Data will be made available on request.

References

[1] A. Sheer, M. Fahad Sardar, F. Younas, P. Zhu, S. Noreen, T. Mehmood, Z. Ur Rahman Farooqi, S. Fatima, W. Guo, Trends and social aspects in the management and conversion of agricultural residues into valuable resources: a comprehensive approach to counter environmental degradation, food security, and climate change, Bioresour. Technol. 394 (2024) 130258, https://doi.org/10.1016/J.BIORTECH.2023.130258.

[2] Q. Jia, G.Qin Liao, L. Chen, Y. Zhong Qian, X. Yan, J. Qiu, Pesticide residues in animal-derived food: current state and perspectives, Food Chem. 438 (2024) 137974, https://doi.org/10.1016/J.FOODCHEM.2023.137974.

[3] M.M.M. Mouiche, N.H. Okah-Nnane, F. Moffo, I. Djibo, N. Pemi Mapiefou, S. E. Mpouam, Y.M. Mfopit, J.P.K. Mingoas, S.F. Tebug, J.A. Ndukum, Antibiotic residues in foods of animal origin in cameroon: prevalence, consumers' risk perceptions, and attitudes, J. Food Prot. 87 (2024) 100237, https://doi.org/10.1016/J.JFP.2024.100237.

[4] M. Yang, Y. Wang, G. Yang, Y. Wang, F. Liu, C. Chen, A review of cumulative risk assessment of multiple pesticide residues in food: current status, approaches and future perspectives, Trends Food Sci. Technol. 144 (2024) 104340, https://doi.org/10.1016/J.TIFS.2024.104340.

[5] S. Munir, A. Azeem, M. Sikandar Zaman, M. Zia Ul Haq, From field to table: ensuring food safety by reducing pesticide residues in food, Sci. Total. Environ. 922 (2024) 171382, https://doi.org/10.1016/J.SCITOTENV.2024.171382.

[6] F.N. Castañeda, R.B. Pellegrino Vidal, J. Aspromonte, Untargeted chromatographic methods coupled with chemometric strategies for the analysis of food and related samples, TrAC Trends Anal. Chem. 173 (2024) 117650, https://doi.org/10.1016/J.TRAC.2024.117650.

[7] P.S. Hew, J. Selamat, N.N. Jambari, S. Murugesu, M. Sanny, A. Khatib, R. Sukor, Quality and safety of food product – Current assessment, issues, and metabolomics as a way forward, Food Chem. Adv. 4 (2024) 100632, https://doi.org/10.1016/J.FOCHA.2024.100632.

[8] R.O. Martins, G.L. de Araújo, C.S. de Freitas, A.R. Silva, R.C. Simas, B.G. Vaz, A. R. Chaves, Miniaturized sample preparation techniques and ambient mass

spectrometry as approaches for food residue analysis, J. Chromatogr. A 1640 (2021) 461949, https://doi.org/10.1016/J.CHROMA.2021.461949.

[9] C. Vakh, M. Tobiszewski, Greenness assessment of analytical methods used for antibiotic residues determination in food samples, TrAC Trends Anal. Chem. 166 (2023) 117162, https://doi.org/10.1016/J.TRAC.2023.117162.

[10] J.C. Cruz, I.D. de Souza, F.M. Lanças, M.E.C. Queiroz, Current advances and applications of online sample preparation techniques for miniaturized liquid chromatography systems, J. Chromatogr. A 1668 (2022) 462925, https://doi.org/10.1016/J.CHROMA.2022.462925.

[11] M. Samadifar, Y. Yamini, M.M. Khataei, M. Shirani, Automated and semi-automated packed sorbent solid phase (micro) extraction methods for extraction of organic and inorganic pollutants, J. Chromatogr. A 1706 (2023) 464227, https://doi.org/10.1016/J.CHROMA.2023.464227.

[12] D.A. Vargas Medina, A.T. Cardoso, E.V.S. Maciel, F.M. Lanças, Current materials for miniaturized sample preparation: recent advances and future trends, TrAC Trends Anal. Chem. 165 (2023) 117120, https://doi.org/10.1016/J.TRAC.2023.117120.

[13] E. Torabi, A. Abdar, N. Lotfian, M. Bazargan, C. Simms, M.A. Moussawi, A. Amiri, M. Mirzaei, T.N. Parac-Vogt, Advanced materials in sorbent-based analytical sample preparation, Coord. Chem. Rev. 506 (2024) 215680, https://doi.org/10.1016/J.CCR.2024.215680.

[14] K.S. Novoselov, A.K. Geim, S.V. Morozov, D. Jiang, Y. Zhang, S.V. Dubonos, I. V. Grigorieva, A.A. Firsov, Electric field in atomically thin carbon films, Science 306 (2004) 666–669, https://doi.org/10.1126/SCIENCE.1102896 (1979).

[15] W.K. Li, Y.P. Shi, Recent advances of carbon materials on pesticides removal and extraction based determination from polluted water, TrAC Trends Anal. Chem. 171 (2024) 117534, https://doi.org/10.1016/J.TRAC.2024.117534.

[16] M.A. Suliman, M. Sajid, M.K. Nazal, M.A. Islam, Carbon-based materials as promising sorbents for analytical sample preparation: recent advances and trends in extraction of toxic metal pollutants from various media, TrAC Trends Anal. Chem. 167 (2023) 117265, https://doi.org/10.1016/J.TRAC.2023.117265.

[17] D.C. da Silva Alves, B. Healy, T. Yu, C.B. Breslin, Graphene-based materials immobilized within chitosan: applications as adsorbents for the removal of aquatic pollutants, Materials 14 (2021) 3655, https://doi.org/10.3390/MA14133655. . (Basel).

[18] D.R. Rout, H.M. Jena, O. Baigenzhenov, A. Hosseini-Bandegharaei, Graphene-based materials for effective adsorption of organic and inorganic pollutants: a critical and comprehensive review, Sci. Total. Environ. 863 (2023) 160871, https://doi.org/10.1016/J.SCITOTENV.2022.160871.

[19] Y. Iqbal, I. Ahmed, M.F. Irfan, S.A.S. Chatha, M. Zubair, A. Ullah, Recent advances in chitosan-based materials; The synthesis, modifications and biomedical applications, Carbohydr. Polym. 321 (2023) 121318, https://doi.org/10.1016/J.CARBPOL.2023.121318.

[20] X. Zang, R. Jiang, H.Y. Zhu, Q. Wang, Y.Q. Fu, D.X. Zhao, J.B. Li, H. Liu, A review on the progress of magnetic chitosan-based materials in water purification and solid-phase extraction of contaminants, Sep. Purif. Technol. 330 (2024) 125521, https://doi.org/10.1016/J.SEPPUR.2023.125521.

[21] K. Mohan, D.K. Rajan, J. Rajarajeswaran, D. Divya, A.R. Ganesan, Recent trends on chitosan based hybrid materials for wastewater treatment: a review, Curr. Opin. Environ. Sci. Health 33 (2023) 100473, https://doi.org/10.1016/J.COESH.2023.100473.

[22] C. Li, F. Li, K. Wang, Q. Wang, H. Liu, X. Sun, D. Xie, Synthesis, characterizations, and release mechanisms of carboxymethyl chitosan-graphene oxide-gelatin composite hydrogel for controlled delivery of drug, Inorg. Chem. Commun. 155 (2023) 110965, https://doi.org/10.1016/J.INOCHE.2023.110965.

[23] B.H. Fumes, F.M. Lanças, Use of graphene supported on aminopropyl silica for microextraction of parabens from water samples, J. Chromatogr. A 1487 (2017) 64–71, https://doi.org/10.1016/J.CHROMA.2017.01.063.

[24] M. Jordan-Sinisterra, F.M. Lanças, Microextraction by packed sorbent of selected pesticides in coffee samples employing ionic liquids supported on graphene nanosheets as extraction phase, Anal. Bioanal. Chem. 414 (2022) 413–423, https://doi.org/10.1007/S00216-021-03245-3.

[25] W.S. Hummers, R.E. Offeman, Preparation of graphitic oxide, J. Am. Chem. Soc. 80 (1958) 1339, https://doi.org/10.1021/Ja01539a017.

[26] E.V.S. Maciel, J.V.B. Borsatto, K. Mejia-Carmona, F.M. Lanças, Application of an in-house packed octadecylsilica-functionalized graphene oxide column for capillary liquid chromatography analysis of hormones in urine samples, Anal. Chim. Acta 1239 (2023) 340718, https://doi.org/10.1016/J.ACA.2022.340718.

[27] E.V.S. Maciel, B.H. Fumes, A.L. de Toffoli, F.M. Lanças, Graphene particles supported on silica as sorbent for residue analysis of tetracyclines in milk employing microextraction by packed sorbent, Electrophoresis 39 (2018) 2047–2055, https://doi.org/10.1002/ELPS.201800051.

[28] F.N. Andrade, A.J. Santos-Neto, D.A.V. Medina, F.M. Lanças, A molecularly imprinted polymer for microextraction by packed sorbent of sulfonylureas herbicides from corn samples, J. Food Compos. Anal. 121 (2023) 105388, https://doi.org/10.1016/J.JFCA.2023.105388.

[29] A.M. Hegazy, R.M. Abdelfatah, H.M. Mahmoud, M.A. Elsayed, Development and validation of two robust simple chromatographic methods for estimation of tomatoes specific pesticides' residues for safety monitoring prior to food processing line and evaluation of local samples, Food Chem. 306 (2020) 125640, https://doi.org/10.1016/J.FOODCHEM.2019.125640.

[30] P. Borman, D. Elder, Q2(R1) Validation of Analytical procedures, ICH Quality Guidelines: An implementation Guide, John Wiley & Sons, Inc., New Jersey, 2017, pp. 127–166.

[31] G. Mastellone, A. Marengo, B. Sgorbini, P. Rubiolo, J.L. Anderson, C. Cagliero, Ultrasound-assisted dispersive solid-liquid microextraction with eutectic solvents for the determination of cannabinoids in different hemp products, J. Chromatogr. B 1232 (2024) 123967, https://doi.org/10.1016/J.JCHROMB.2023.123967.

[32] Y. Shi, G. Song, A. Li, J. Wang, H. Wang, Y. Sun, G. Ding, Graphene oxide-chitosan composite aerogel for adsorption of methyl orange and methylene blue: effect of pH in single and binary systems, Colloids. Surf. A Physicochem. Eng. Asp. 641 (2022) 128595, https://doi.org/10.1016/J.COLSURFA.2022.128595.

[33] W.M.A. El Rouby, A.A. Farghali, M.A. Sadek, W.F. Khalil, Fast removal of Sr(II) from water by graphene oxide and chitosan modified graphene oxide, J. Inorg. Organomet. Polym. Mater. 28 (2018) 2336–2349, https://doi.org/10.1007/S10904-018-0885-9.

[34] I. Silvestro, C. Ciarlantini, I. Francolini, P. Tomai, A. Gentili, C. Dal Bosco, A. Piozzi, Chitosan–graphene oxide composite membranes for solid-phase extraction of pesticides, Int. J. Mol. Sci. 2021 (22) (2021) 8374, https://doi.org/10.3390/IJMS22168374.

[35] L. Shao, X. Chang, Y. Zhang, Y. Huang, Y. Yao, Z. Guo, Graphene oxide cross-linked chitosan nanocomposite membrane, Appl. Surf. Sci. 280 (2013) 989–992, https://doi.org/10.1016/J.APSUSC.2013.04.112.

[36] S. Peng, Y. Huang, S. Ouyang, J. Huang, Y. Shi, Y.J. Tong, X. Zhao, N. Li, J. Zheng, J. Zheng, X. Gong, J. Xu, F. Zhu, G. Ouyang, Efficient solid phase microextraction of organic pollutants based on graphene oxide/chitosan aerogel, Anal. Chim. Acta 1195 (2022) 339462, https://doi.org/10.1016/J.ACA.2022.339462.

[37] K. Ebisike, A.E. Okoronkwo, K.K. Alaneme, Synthesis and characterization of chitosan–silica hybrid aerogel using sol-gel method, J. King Saud. Univ. Sci. 32 (2020) 550–554, https://doi.org/10.1016/J.JKSUS.2018.08.005.

[38] L.S. Mokoena, J.P. Mofokeng, Synthesis and characterization of graphene oxide (GO) for the removal of lead ions in water, Carbon Trends 15 (2024) 100339, https://doi.org/10.1016/J.CARTRE.2024.100339.

[39] Z. Zhang, H.C. Schniepp, D.H. Adamson, Characterization of graphene oxide: variations in reported approaches, Carbon 154 (2019) 510–521, https://doi.org/10.1016/J.CARBON.2019.07.103. . N. Y..

[40] N.T.T. Dang, T.T.L. Chau, H. Van Duong, H.T. Le, T.T. Van Tran, T.Q. Le, T.P. Vu, C.D. Nguyen, L.V. Nguyen, T.D. Nguyen, Water-soluble chitosan-derived sustainable materials: towards filaments, aerogels, microspheres, and plastics, Soft Matter 13 (2017) 7292–7299, https://doi.org/10.1039/C7SM01292F.

[41] Y. Gong, Y. Yu, H. Kang, X. Chen, H. Liu, Y. Zhang, Y. Sun, H. Song, Synthesis and characterization of graphene oxide/chitosan composite aerogels with high mechanical performance, Polymers 11 (2019) 777, https://doi.org/10.3390/POLYM11050777. . (Basel).

[42] Q. Wu, W. Wu, X. Zhan, X. Hou, Three-dimensional chitosan/graphene oxide aerogel for high-efficiency solid-phase extraction of acidic herbicides in vegetables, New Chem. 44 (2020) 10654–10661, https://doi.org/10.1039/D0NJ01960G.

[43] H. Chi, G. Liu, Carbon nanomaterial-based molecularly imprinted polymer sensors for detection of hazardous substances in food: recent progress and future trends, Food Chem. 420 (2023) 136100, https://doi.org/10.1016/J.FOODCHEM.2023.136100.

[44] E.V.S. Maciel, K. Mejía-Carmona, M. Jordan-Sinisterra, L.F. da Silva, D.A. Vargas Medina, F.M. Lanças, The Current role of graphene-based nanomaterials in the sample preparation arena, Front. Chem. 8 (2020) 553150, https://doi.org/10.3389/FCHEM.2020.00664/BIBTEX.

[45] A. Nasiri, R. Jahani, S. Mokhtari, H. Yazdanpanah, B. Daraei, M. Faizi, F. Kobarfard, Overview, consequences, and strategies for overcoming matrix effects in LC-MS analysis: a critical review, Analyst 146 (2021) 6049–6063, https://doi.org/10.1039/D1AN01047F.

[46] Agência Nacional de Vigilância Sanitária - ANVISA, Monografia de agrotóxicos. https://www.gov.br/anvisa/ptbr/acessoainformacao/dadosabertos/informacoes-analiticas/monografias-de-agrotoxicos, 2021 (accessed 16 July 2024).

[47] European Food Safety Authority - EFSA, https://eur-lex.europa.eu/homepage.html, 2024 (accessed 16 July 2024).

[48] J. Werner, A. Zgoła-Grześkowiak, T. Grześkowiak, R. Frankowski, Biopolymers-based sorbents as a future green direction for solid phase (micro)extraction techniques, TrAC Trends Anal. Chem. 173 (2024) 117659, https://doi.org/10.1016/J.TRAC.2024.117659.

[49] F.N. Andrade, A.H. Ide, N.D.R. Neng, F.M. Lanças, J.M.F. Nogueira, Determination of trace levels of triazines in corn matrices by bar adsorptive microextraction with a molecularly imprinted polymer, J. Sep. Sci. 39 (2016) 756–761, https://doi.org/10.1002/JSSC.201501101.

[50] A. Abbasalizadeh, M. Ghalkhani, E.M. Khosrowshahi, A. Mazani, A. Hosseini, E. Sohouli, F. Ahmadi, Determination of selected pesticides by GC-FID after CNO/MOF nanocomposites-based dispersive solid phase extraction coupled with liquid microextraction, Diam. Relat. Mater. 137 (2023) 110087, https://doi.org/10.1016/J.DIAMOND.2023.110087.

[51] H. Sereshti, S.S. Jazani, N. Nouri, G. Shams, Dispersive liquid–liquid microextraction based on hydrophobic deep eutectic solvents: application for tetracyclines monitoring in milk, Microchem. J. 158 (2020) 105269, https://doi.org/10.1016/J.MICROC.2020.105269.

[52] Y. Wang, M. He, B. Chen, H. Cao, Y. Liang, B. Hu, Porous organic framework as coating for stir bar sorptive extraction of carbamate pesticides from corn and potato samples, Food Chem. 397 (2022) 133785, https://doi.org/10.1016/J.FOODCHEM.2022.133785.

[53] E.M. Khosrowshahi, M.R.A. Mogaddam, M.A. Farajzadeh, M. Nemati, Magnetic silicon carbide nanocomposite as a sorbent in magnetic dispersive solid phase extraction followed by dispersive liquid–liquid microextraction in the gas chromatographic determination of pesticides, Microchem. J. 181 (2022) 107786, https://doi.org/10.1016/J.MICROC.2022.107786.

[54] A. Mohebi, M. Samadi, H.R. Tavakoli, K. Parastouei, Homogenous liquid–liquid extraction followed by dispersive liquid–liquid microextraction for the extraction

of some antibiotics from milk samples before their determination by HPLC, Microchem. J. 157 (2020) 104988, https://doi.org/10.1016/J.MICROC.2020.104988.